Effect of size of air holes and width of flat on NR-PC flat lens for target detection and image

J. LU[a*], Y. SHEN[b,c], Y.F. LIAN[d]
[a]*Lab Management and Service Center, University of Shanghai for Science and Technology, Shanghai 200093, China*
[b]*Shanghai Medical instrumentrtion college, Shanghai 200093, China*
[c]*University of Shanghai for Science and Technology, Shanghai 200093, China*
[d]*School of Computer Science and Communication Engineering, Jiangsu University, Zhenjiang, 212013, China*

A finite-difference time-domain (FDTD) method is used to investigate the effect of the size of air holes and width of flat of cylinder air holes negative-refraction photonic crystal (NR-PC) lens on the performance of lightwave target detection and imaging in the paper. Numerical simulations indicate that significant enhancement of the scattering signal can be obtained due to the use of the NR-PC flat lens; consequently, great improvement of the refocusing gain as well as the imaging resolution will be provided. We further study the effect on target detection and imaging by using different size of air holes and width of flat of NR-PC flat lens. The results demonstrate that we can get better resolution by appropriately decreasing the radius of the defective cylinder (R=0.2*a*). What's more, the narrower the width (from seven rows to eleven rows air holes) of flat is, the lower the refocusing resolution will be.

(Received May 23, 2013; accepted January 21, 2015)

Keywords: NR-PC, Cylinder air holes, Dynamic scanning, Refocusing resolution

1. Introduction

Negative-refraction materials, as a new kind of artificial electromagnetic media, have attracted great interest in recent years. Negative-refraction materials with both negative refractivity and negative permeability are usually known as left-handed materials (LHM), since the electric field vector, the magnetic field vector and the wave vector of electromagnetic wave form a left-handed triplet in LHM. In the year of 1968, V.G. Veselago investigated the anomalous phenomena of electromagnetic wave propagating in LHM theoretically [1], and then in 2000 D. R. Smith et al demonstrated firstly such LHM in microwave band in their laboratory [2].

Basing on abnormal electromagnetic properties in LHM, LHM have found many important implications, such as, photolithography and nuclear magnetic resonance (NMR) as well as imaging [3-11]. Among these applications of the LHM, focusing with lenses having flat surfaces has been proposed [5].Theoretical analysis and numerical simulations [6] indicated that, the so-called perfect lens made of LHM with no losses may achieve a focus resolution overcoming the optical diffraction limit. And generally, the higher focus resolution yields the better imaging resolution [7].

Although the flat LHM lens could be used as a 'perfect lens' for near focusing beyond the diffraction limit in theory, there is still much uncertainty about whether such materials actually existed in nature. By using a different method, M. Notomi has demonstrated 2D photonic crystals exhibiting negative-index or negative-refraction effects [12]. From their results we know that negative refraction usually occurs in the band gap of the equifrequency surface (EFS) in $\boldsymbol{k}$ space because the size of the contour of EFS in the $\boldsymbol{k}$ space decreases with increasing frequencies. And the contour of EFS up to a certain frequency takes the shape of a quasi-circular [13], which means that the light propagating in PC is similar to that propagating in the isotropic medium at these frequencies. Thereby an effective negative index of refraction n_{eff} can be used to describe the propagation property of light with frequency falling into a certain frequency spectrum for a given NR-PC, and the NR-PC could be used as a flat LHM.

Based on the phenomena of negative refraction, it is easy to envision that the NR-PC flat lens and the LHM flat lens [5] share the same image-forming principle.

As shown in Fig. 1 (a), lightwave emitted from a point source on one side of the NR-PC lens can be focused at one focal point F_1 inside the NR-PC lens firstly, and then be focused at the other focal point F_2 outside the NR-PC lens. When a target is brought into the focal point F_2, lightwave from the source is focused on the target by the flat NR-PC lens, and the target will backscatter the focused lightwave(obtain the scattered field), then the backscattered lightwave will be refocused in the vicinity of the source point by the same flat NR-PC lens. Since the focal point F_2 can be controlled easily by moving the point

source along the lines of the surface of lens or adjusting the distance between them, the target can be scanned easily and its image in the vicinity of the source point is enhanced significantly. Generally, the complete lightwave recorded at each receiving point is actually the compound of three parts, i.e., the wave emitted from the source, the wave reflected from the entrance and exit surfaces of NR-PC lens (for NR-PC of $n_{\text{eff}}\neq$-1), and the refocused wave of the backscattered lightwave (scattering signal). Thus, the scattering signal is achievable by taking the difference between what is recorded by the detector with/without a target on the focal point F_2. This means that target detection and imaging could be realized, with high resolution ratio and without complicated imaging algorithm, just by computing the lightwave distribution of the scattering signal from the target [6], as shown in Figs.1 and 2(a). For a medium with negative index or negative-refraction effects, the image existing outside of the medium is formed through light waves from target experiencing negative refraction at its two interfaces. Therefore, NR-PC could be used in the optical-wave target detection and imaging, and the imaging of the NR-PC slab also obeys geometrical optics [14, 15].

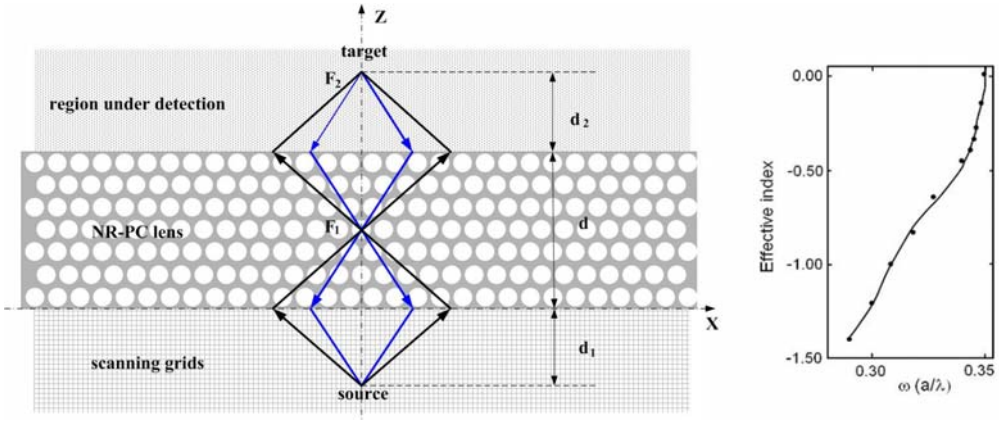

Fig. 1. (a) Target detection and imaging by using NR-PC flat lens; (b) Change curve of n_{eff} and ω in the NR-PC lens (for TM mode).

The two-dimensional photonic crystal structure examined in this paper, as shown in Fig. 1 (a), is formed by periodically drilling 7 rows (along the Z-axis) of identical air holes with 30 air holes (along the X-axis) in each row in a GaAs matrix with dielectric constant ε=12.96 (n=3.6). And the air cylinders take on a triangular array, here the radius of the air cylinders is 0.4a (a represents the lattice constant). The effective refractive index of the photonic crystal is calculated with TM mode and is drawn in Fig. 1 (b) by using the algorithm in reference of [8]. It is understandable that n_{eff} changes with normalized frequency $\omega=a/\lambda$. From Fig. 1 (b), we know that, when n_{eff} takes the value of -1, the corresponding normalized frequency ω is about 0.3068.

In this paper, we mainly discuss the influence of different radius of air holes and width of flat for NR-PC flat lens on the performance of lightwave target detection and imaging system. Numerical simulations with the finite-difference time-domain (FDTD) method show that significant enhancement of the scattering signal can be obtained due to the use of the NR-PC flat lens; consequently, great improvement of the refocusing gain as well as the imaging resolution will be provided. Detailed comparison between the scattering signals obtained with and without use of the NR-PC lens will be more helpful to evaluate flat NR-PC lens' specific application on target detection and imaging. Then we change the radius of the air holes of NR-PC flat lens. By using dynamic scanning scheme, we find that it could improve the lateral resolution of target scanning through appropriately decreasing the radius of the defective cylinder (R=0.2a). In addition, we also study

2. Design and calculation models of the NR-PC flat lens

The Maxwell's equations in the photonic crystals can be written as

$$\frac{\partial \boldsymbol{H}}{\partial t} = -\frac{1}{\mu_0 \mu(r)} \nabla \times \boldsymbol{E} , \tag{1}$$

$$\frac{\partial \boldsymbol{E}}{\partial t} = \frac{1}{\varepsilon_0 \varepsilon(r)} \nabla \times \boldsymbol{H} , \tag{2}$$

where $\nabla = \frac{\partial}{\partial x}\boldsymbol{i} + \frac{\partial}{\partial y}\boldsymbol{j} + \frac{\partial}{\partial z}\boldsymbol{k}$ is the Hamiltonian operator, $\boldsymbol{E}$ and $\boldsymbol{H}$ are the electric and magnetic field vectors of the electromagnetic wave, the permittivity $\varepsilon(r)$ is the relative dielectric constant, and $\mu(r)$=1 is the relative magnetic

permeability.

The FDTD method [13] is well-established with a somewhat lower computational capacity in comparison to its high accuracy when compared with other methods. It has been widely used to study characteristics of electromagnetic waves in NR-PC. Its fundamental principle is that Maxwell's equations are first expressed as scalar equations of electric and magnetic field components in Cartesian coordinates, and then the differential quotient is replaced with the difference quotient with accuracy to the second order. In our simulation, a perfectly matched layer (PML) is used in the ***X*** and ***Y*** directions as boundary conditions [13]. Because these equations are functions of space and time, they can be discretized in the space and time domains by the Yee-cell technique and be used to find field solutions numerically.

It is noteworthy that the mode of light propagating in photonic crystals (PC) is very different from that in LHM. For the LHM with refractive index $n = -1$, there is no reflection at the air-LHM interface, however light will experience multiple reflection and refraction at the air-PC interface, even for NR-PC when $n_{eff} = -1$, leading to great losses or much lower transmissivity for the light propagating through the NR-PC. To optimize the performance of the focus-scanning scheme, an effective way to improve transmissivity is needed.

The corresponding investigation of raising the transmissivity has already been presented in our previous thesis cited by OPTIK [17]. When the center frequency (ω_p) of the wave source is set at $0.3068(a/\lambda)$, the transmission is enhanced dramatically, with the transmission coefficient up to 4500 at the frequency point of $0.3068(a/\lambda)$. The physical mechanism can be explained by the redistribution of optical energy. The incident optical waves with a different frequency will experience intensive Bragg scattering when they are incident upon the NR-PC and propagating in the NR-PC because of the periodic distribution of negative-refraction media, which results in mini-forbidden bands and a photonic tunneling effect for a given NR-PC [18, 19]. At the same time, the optical energy is highly localized, and the high transmissivity appears at the resonance frequency.

3. Refocusing of the backscattered wave in target detection and imaging from an NR-PC flat lens

The focusing-refocusing property is a very important performance parameter that supports the use of the NR-PC flat lens for lightwave target detection and imaging. By taking the measured Full Width Half Maximum (FWHM) for the given energy carried by the focused Beam [16] or the width at 0.707-maximum of the normalized field intensity of the refocused beam profile as the definition of resolution, the performance of the target detection and imaging system based on the NR-PC flat lens can be further evaluated. In particular, for the detection and imaging of a small target at an early stage, high sensitivity is very desirable, thus, our investigation may have great significance for imaging systems.

In our FDTD simulations, we consider a typical detecting and imaging system, which consists of a point source-detector pair and a flat NR-PC lens, and the center frequency of the point source is adjusted to $0.3068(a/\lambda)$ for a high transmissivity. Meanwhile, the source-detector pair were set to move together along the scanning line $z = -\lambda$ with intervals of $\Delta x = 0.2\ um$. The 2D flat NR-PC lens with a width of $d = 2\lambda$ is set at $0 \le z \le 2\lambda$, and a target of a PEC square with a side length of $L = 1/3\lambda$ is located at the focal point F_2

First the performance of the complete lightwave is investigated. The simulation diagram of the complete lightwave field in the computation area and its corresponding field intensity distribution along the scanning line $z = -\lambda$ are depicted in Fig. 2 (a) and (b).

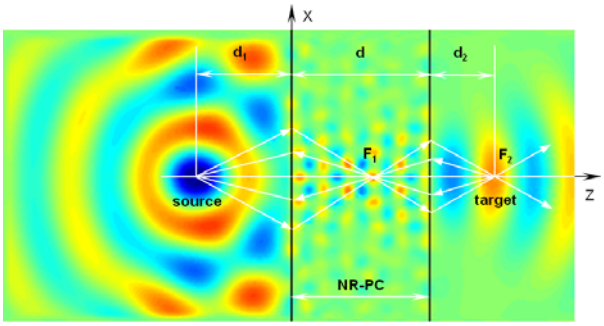

(a)

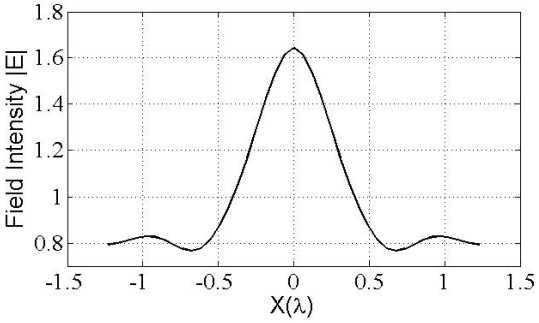

(b)

Fig. 2. (a) Simulation diagram of the complete lightwave in the computation area (b) Lateral beam profile of the total field intensity along line $z = -\lambda$.

From the arrowheaded lines in Fig. 2(a), it is clear that the imaging of the NR-PC lens obeys geometrical optics. Furthermore, there is a one-to-one correspondence between the energy distribution of the complete lightwave field (Fig. 2 (a)) and the distribution curve of its field intensity (Fig. 2(b)), and the maximum field intensity on

the line $z = -\lambda$ is obtained in the vicinity of the point source.

Fig. 2 depicts the properties of the complete lightwave, whereas the main role of NR-PC flat lens in target detection and imaging is actually embodied in the characteristics of the scattering signal from the target. Therefore, to obtain the scattering wave, we may substrate the fields recorded under situation without the target at F_2 from the fields recorded under situation with the target at F_2.

For further comparison, we also investigate the detection system without using the NR-PC lens. Detailed comparison of the scattering signal obtained with and without the use of the NR-PC lens when $\omega_p = 0.3068(a/\lambda)$ is shown in Fig. 3. The results show that due to the use of the NR-PC lens, the refocusing resolution equals approximately to 0.3718λ, which is at least fourfold improvement if compared to 1.6186λ (the refocusing resolution of the directly scattering signal without using the NR-PC lens).

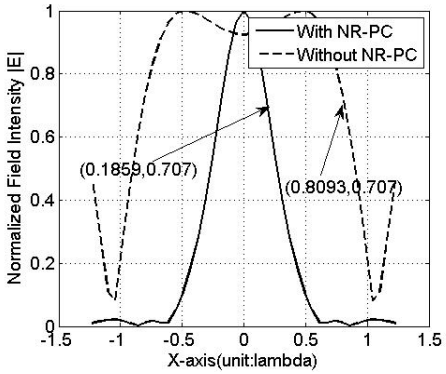

Fig. 3 Beam profile of the normalized field intensity of the scattering signal obtained by detecting the square target of $L=1/3\lambda$ with and without the NR-PC flat lens when $\omega_p = 0.3068(a/\lambda)$.

From Fig. 3 we may have the conclusion that there is significant improvement in the scattering signal, which is attributable to the use of the NR-PC lens. It is intelligible from the standpoint of theory of the mini-forbidden band and resonance excitation effect, as well as the focusing characteristics of the NP-PC lens and the exponential amplification of the evanescent wave [17, 18].

4. The influence of the size of air holes of NR-PC flat lens on target detection and imaging system

It has been demonstrated that the refocusing resolution will be improved due to the use of NR-PC lens. Further research should be done to find the other factors which will affect the image resolution. Thus, we change the size of air holes in NR-PC flat lens.

Because the structure of NR-PC flat lens has been changed, the corresponding normalized frequency constant ω is not about 0.3068, when n_{eff} takes the value of -1. Firstly, we should find normalized frequency constant (when $n_{eff} = -1$).

To further study the importance of NR-PC flat lens in target detection and imaging system, we change the radius of air holes of NR-PC flat lens. Setting the radii of air holes to $0.1a$, $0.2a$, $0.3a$ respectively, while keeping the other parameters the same with perfect lens, we can get the corresponding beam profiles of the normalized field intensity of the scattering signals based on the structure for target detection and imaging, which shown in Fig. 4 and Table 1.

Table 1. Comparison of the refocusing resolution of the NR-PC flat lens with different radii of air holes.

radius	R=0.1a	R=0.2a	R=0.3a	R=0.4a
normalized frequency constant (when $n_{eff} = -1$)	$0.2609(a/\lambda)$	$0.2637(a/\lambda)$	$0.2733(a/\lambda)$	$0.3068(a/\lambda)$
resolution	0.6088λ	0.3268λ	0.3836λ	0.3718λ

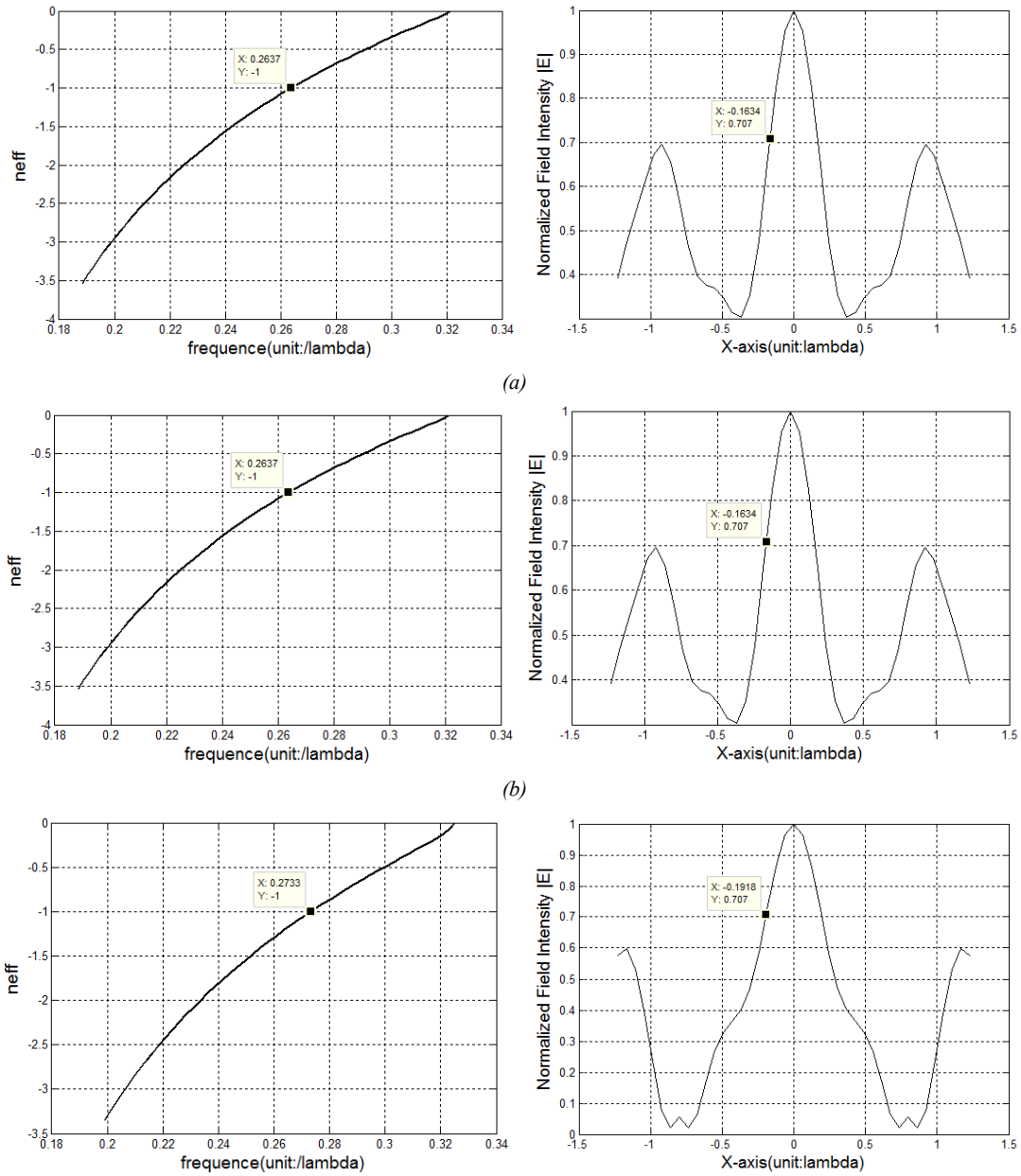

Fig. 4. Left Change curve of n_{eff} and ω in the NR-PC lens; right Normalized field intensity of the refocused beam. The radii of air holes are 0.1a (a), 0.2a (b), and 0.3a (c) in NR-PC flat lens.

From Fig. 4 and Table 1, we have the observation that the refocusing resolution is different when we use NR-PC flat lens with different radius to detect the same square target (L=1/3λ). The refocusing resolution (0.3268λ) of R=0.2a is best in the above. There is approximately 0.045λ improvement in the refocusing resolution, when compared to 0.3718λ obtained from the detection of same target with the R=0.4a. The results show that we can get better resolution by appropriately decreasing the radius of the defective cylinder (R=0.2*a*).

5. The influence of the width of flat of NR-PC flat lens on target detection and imaging system

We mainly study the influence of the radius of air holes of NR-PC flat lens on target detection and imaging system in the previous section. In order to further research the effect of NR-PC flat lens on target detection and imaging system, we change the width of flat in the following.

We also use the two-dimensional structure (Fig. 1(a)),

which is formed by periodically 7 rows (along the Z-axis) of identical air holes with 30 air holes (along the X-axis) in each row in GaAs matrix. And the air cylinders take on a triangular array; here the radius of the air cylinders is 0.4*a*. To study the influence of the width of flat on resolution, we etch 7, 8, 9, 10, 11 rows air holes in X-axis respectively (the GaAs matrix change also), while maintain 30 column in Z-axis. The center frequency (ωp) of the wave source is also set at 0.3068(a/λ). With the same way like last section, the square target with length of L=1/6λ is detected by these NR-PC flat lens. With dynamic scanning system, the corresponding beam profiles of the normalized field intensity of the scattering signals are presented in Fig. 5, and the refocusing resolution date are shown in Table 2.

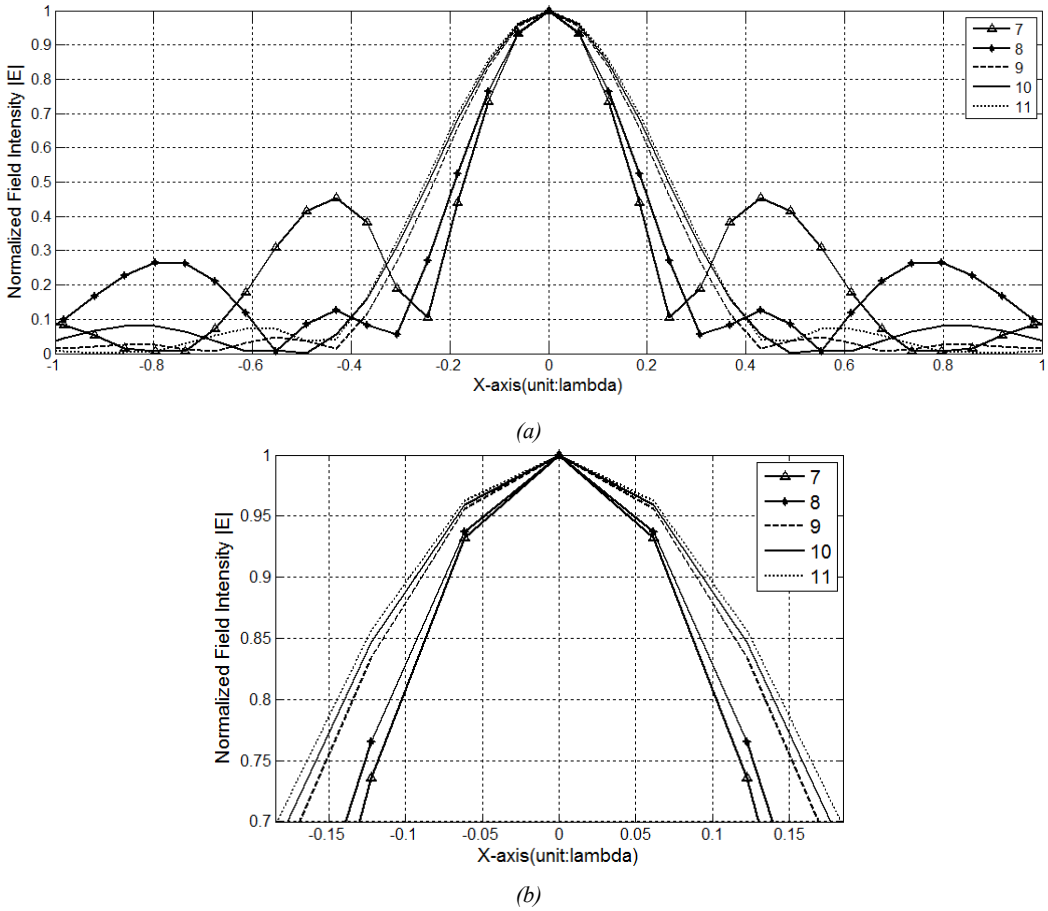

Fig. 5. the normalized field intensity obtained by different width of flat (7, 8, 9,10, 11 row air holes); (a) the complete figure (b) the partial figure.

Table 2. the refocusing resolution obtained by 7-11 row air holes.

NR-PC flat lens	7 row	8 row	9 row	10 row	11 row
resolution	0.2572λ	0.2752λ	0.3338λ	0.3496λ	0.3624λ

From Fig. 5 and Table 2, we have the observation that the refocusing resolution obtained by NR-PC flat lens is getting worse when increasing the number of air holes. That means the refocusing resolution of NR-PC flat lens get worse with the increase of width of flat. This obviously conforms to the general laws of physics. With the wider of flat, the light transmission time in flat is longer and the loss of light transmission is greater. So the refocusing resolution will reduce.

5. Conclusions

In this paper we main applied dynamic scanning system and 2D FDTD method to study the influence of the size of air holes and width of flat of cylinder air holes negative-refraction photonic crystal (NR-PC) lens on the performance of lightwave target detection and imaging. Owing to the influence of the mini-forbidden band and resonance excitation effect, high transmissivity will appear at the resonance frequency when the lightwave goes through the NR-PC lens. What's more, the focusing characteristics of the NR-PC lens and the exponential amplification of the evanescent wave [3] make the scheme quite efficient in raising the backscattered wave, which leads to a refocusing resolution and imaging resolution with significant enhancement. Further study show that we can get better resolution by appropriately decreasing the radius of the defective cylinder (R=0.2*a*). Moreover, the narrower the width (from seven rows to eleven rows air holes) of flat is, the lower the refocusing resolution will be.

In conclusion, our investigation optimizes the performance of the focus-scanning scheme, and provides the basis for converting idealized LHM lens into physically realizable NR-PC flat lens.

References

[1] V. G. Vesolago, Sov Phys Usp, **10**(4),509D(1968).
[2] D. R. Smith, N. Kroll, Phys Rev Lett, **85**(l4), 2933D(2000).
[3] J. B. Pendry, Phys Rev Lett, **85**(18), 3966(2000).
[4] J. T. Shen, P. M. Platzman, Appl. Phy Lett, **80**(18), 3286D(2002)
[5] S. A. Cummer, Appl Phy Lett, **82**(10), 1503D(2003).
[6] X. S. Rao, C. K. Ong, Phys Rev E, **68**(6), 067601(2003).
[7] G, Wang. J. R. Fang, X. T. Dong, Opt Expr, **15**(6), 3312D(2007).
[8] G, Wang, J. R Fang, X. T. Dong, IEEE Trans Antennas Propog, **55**(12), 3534D(2007).
[9] M. Notomi, Phys Rev B, **62**(16), 10696D(2000).
[10] K. Guven, K. Aydin, K. B. Alici et al., Phys Rev B, **70**(20), 205125D(2004).
[11] Y. T. Fang H. J. Sun, T. G. Shen, Opt Materials, **28**(10), 1156D(2006).
[12] Y. T. Fang, T. G. Shen, Chin Phys Lett, **22**(4), 949D(2005).
[13] K. S. Yee, IEEE Trans Antennas Propog, **14**(3), 302(1966).
[14] Q. Min, S. L. He, Phys Rev B, **61**(19), 12871D(2000).
[15] X. T. Dong, X. S. Rao, Y. B. Gan et al., IEEE Micr Wirel Comp lett, **14**(6), 301D(2004).
[16] A. Sharon, A. A. Friesem, D. Rosenblatt, Appl. Phys. Lett., **69**, 4154(1997).
[17] I. V. Shadrivov, A. A. Sukhorukov, Y. S. Kivshar, Physical Review E , **6**9, 016617-9(2004).
[18] A. Grbic, G. V. Eleftheriades, Phys Rev Lett, **92**(11), 117403(2004).

*Corresponding author: 938489435@qq.com